Z. Phys. D – Atoms, Molecules and Clusters 2, 319–326 (1986)

Atoms, Molecules and Clusters
Zeitschrift für Physik D
© Springer-Verlag 1986

Autoionization in Diatomic Molecules: An Example of Electrostatic Autoionization in CO

G. Raşeev
Laboratoire de Photophysique Moléculaire*, Université de Paris-Sud, Orsay, France

B. Leyh**
Département de Chimie Générale, Université de Liège, Sart-Tilman par Liège, Belgium

H. Lefebvre-Brion
Laboratoire de Photophysique Moléculaire*, Université de Paris-Sud, Orsay, France

Received March 20, 1986

A review is presented of the different types of autoionization which have been studied theoretically in diatomic molecules: electronic (or electrostatic), rotational, spin-orbit and vibrational autoionizations. An example involving a large number of vibrational channels, is treated. It concerns the electrostatic autoionization in the 730–708 Å wavelength region which appears in the CO photoionization spectrum. The structure observed at 721 Å is explained by the enhancement in intensity of numerous levels of Rydberg series converging to excited vibrational levels of the $A^2\Pi$ state caused by two autoionized Rydberg levels with a $B^2\Sigma^+$ core.

PACS: 33.80E

1. Introduction

Many review papers [1–3] on the photoionization in diatomic molecules have recently appeared. This is due to the large progress in experiment and theory made in the last ten years. In this paper, attention is focused on the autoionization (or preionization) resonances. Since the review of Dehmer et al. [1a] appeared, numerous theoretical results on this subject have been obtained but no global discussion of different types of molecular autoionizations has been presented.

The resonances in the photoionization spectra manifest themselves by peaks in the cross section with a characteristic width. They form two main classes: the shape resonances which are reviewed in this same issue [4] and the autoionization resonances. The shape resonances are expected to be broader than the autoionization ones but experimentally it can be difficult to distinguish between them. Sometimes the autoionization peaks are very broad probably because they correspond to valence states (e.g. in N_2 [5] or in polyatomic molecules [6]) for which the autoionization rate can be very strong.

Theoretically, an easy distinction can be made: the shape resonances correspond to a one-electron process and appear as a consequence of a centrifugal barrier in the electron-ion interaction potential. These resonances can be described by a one state potential model. In contrast, the autoionization or Feshbach resonances appear if a short-range interstate interaction is turned on. The simplest model to describe the autoionization is a two-state model, one bound state and one continuum state corresponding to different ionic states coupled in a configuration interaction picture. In molecules, it is then necessary to go beyond the Born-Oppenheimer approximation as will be explained later.

* Laboratoire du CNRS associé à l'Université Paris-Sud
** Aspirant du Fonds National Belge de la Recherche Scientifique

In the next section, the different types of molecular autoionization will be defined in this simple two-state model. Then, the various theories currently applied to the molecular autoionization will be reviewed and emphasis will be given to the electronic (or electrostatic) autoionization as illustrated by an example from the CO photoionization spectrum. Finally, a discussion of what we can learn from experiment and theory will be given.

2. Different Types of Autoionization Defined in a Two State Model

Photoionization corresponds to the following process,

$$AB+h\nu \rightarrow AB^+ + e^-(k^2 l\lambda)$$

The AB^+ ion is characterized by its electronic, vibrational and rotational state whereas the ejected electron is characterized by its kinetic energy, $k^2/2$ and the quantum numbers l and λ, that correspond to its electronic angular momentum and its projection on the internuclear axis respectively. The whole of the AB^+ ion plus the ejected electron constitutes an ionization continuum, called, in scattering theory language, a channel. For a given $h\nu$, one measures either the amount of absorbed light, or the number of ions formed, or the number of ejected electrons as a function of their kinetic energy. For a given final state of the ion and a given photoelectron kinetic energy, the number of ejected electrons is proportional to the partial photoionization cross section.

Autoionization corresponds to the following indirect photoionization process:

$$AB+h\nu \rightarrow AB^{**} \rightarrow AB^+ + e^-(k^2 l\lambda)$$

where AB^{**} is a superexcited state which is autoionized in the continuum of the AB^+ ion and which manifests itself by a sharp variation in the cross section.

Theoretically, the direct and indirect processes discussed above have to be considered simultaneously. In the framework of Fano's configuration mixing theory [7], the corresponding photoionization cross section σ is expressed as:

$$\sigma \sim \langle \Psi_E |\mu| \Phi_0\rangle^2 = \langle \Phi_E |\mu| \Phi_0\rangle^2 \frac{(q+\varepsilon)^2}{1+\varepsilon^2} \qquad (1)$$

where ψ_E is the configuration interaction continuum wave function which is an eigenfunction of the total Hamiltonian and Φ_E is the continuum, or open channel, (corresponding to $AB^+ + e^-$), wave function which interacts with the discrete resonant Φ_r state (corresponding to AB^{**}) and Φ_0 is the initial state (corresponding to AB). In Eq. (1), q is the profile index, i.e.,

$$q = \frac{1}{\pi} \frac{\langle \Phi_r |\mu| \Phi_0\rangle}{\langle \Phi_E |\mu| \Phi_0\rangle \langle \Phi_r |H| \Phi_E\rangle}$$

and $\varepsilon = (E-E_r)/(\Gamma/2)$ where E_r is the resonance energy and Γ the resonance width.

$$\Gamma = 2\pi \langle \Phi_r |H| \Phi_E\rangle^2 = 2\pi V_{rE}^2 \qquad (2)$$

is proportional to the interaction between the resonant and the energy normalized continuum states. The integrals $\langle \Phi_r |\mu| \Phi_0\rangle$ and $\langle \Phi_E |\mu| \Phi_0\rangle$ are the transition moments from the initial Φ_0 to the final discrete Φ_r and continuum Φ_E functions respectively. From (1) we see that the background continuum cross section, proportional to $|\langle \Phi_E |\mu| \Phi_0\rangle|^2$, is modified by a factor which changes dramatically near the resonance when ε approaches zero and has a maximum at $\varepsilon = 1/q$. If the profile index q is equal to infinity (if for example the transition to the continuum state is zero), the cross section has a Lorentzian profile in the vicinity of the resonant state with a full width at half maximum (FWHM) equal to Γ defined above and related to the lifetime of the resonant state. This situation corresponds to the well known Fermi-Wentzel Golden Rule.

In molecules, the wave functions Φ_E and Φ_r must be introduced in Fano's formulation [8] as Born-Oppenheimer products of the electronic, vibrational and rotational functions,

$$\Phi = \varphi_{el}(r, R)\, \chi_{vib}(R)\, \Theta_{rot}(\hat{R})$$

Here r stands for all electron coordinates and R and $\hat{R}$ the radial and angular part of R. Following the nature of the coupling V_{rE} between wave functions, different types of molecular autoionizations can be defined: electronic, rotational, spin-orbit and vibrational autoionizations (see also [9]).

2.1. Electronic Autoionization

This autoionization appears between states of the same symmetry (same values of Λ, Σ and S which are, respectively, the projection of the angular and spin electronic momentum on the internuclear axis and the spin momentum). Let us consider Rydberg series converging to a vibrational level of an excited electronic state of the ion and autoionized by the continuum state of the same symmetry (described by the wave function Φ_E) of a vibrational level of lower

(or even the ground) state of the ion. Each of these states can be considered as a *diabatic* state, that is to say, an approximate solution of the electronic Hamiltonian. The residual interaction between them is due to the electrostatic terms neglected in this approximation. Consequently, this type of autoionization can be called electrostatic autoionization. This interaction is expected to be rather strong in the particular case where the two electronic ionic states differ only by their multiplicity. An example are the $^3\Sigma_u^-$ Rydberg states converging to the $B^2\Sigma_g^-$ state of O_2^+ and autoionizing in the $^3\Sigma_u^-$ continuum of the $b^4\Sigma_g^-$ state [10]. The width is of 0.2 eV as the two ionic states $B^2\Sigma_g^-$ and $b^4\Sigma_g^-$ originate in the same configuration. For light molecules, except H_2 and Na_2, the electronic autoionization is the most common type of interaction. For electrostatic autoionization, the inclusion of vibration is, in principle essential, because the pair of resonant and continuum states (with the wave functions Φ_r and Φ_E) belong to different electronic ion cores. We have

$$\langle \Phi_r | H | \Phi_E \rangle = \langle \varphi_{el}^r | H | \varphi_{el}^E \rangle \langle \chi_v^r | \chi_v^E \rangle$$

This Condon factorization is possible if H is assumed to be independent of R.

2.2. Rotational Autoionization

In the Born-Oppenheimer approximation, the separation of the rotational coordinates is possible only if certain parts of the rotational Hamiltonian are neglected. These terms can be written:

$-B(J^+L^- + J^-L^+)$ for the L^- uncoupling part

$-B(J^+S^- + J^-S^+)$ for the S^- uncoupling part

where J^+, L^+, S^+ (and, J^-, L^-, S^-) are respectively the raising and lowering operators of the total, electronic and spin angular momenta.

The L-uncoupling part couples the $^1\Sigma_u^+$ and $^1\Pi_u$ Rydberg states of H_2 and consequently will give rise to the autoionization of, for example, the $26p_2$, $v=1$ state of H_2, associated with the $N^+=2$ rotational limit of the ground state of H_2^+, by the $N^+=0$ continuum of this same state [11].

The S-uncoupling part couples the $^3\Pi_0$ component of a $\pi^3 n\sigma$ Rydberg state, associated with the $^2\Pi_{1/2}$ limit of the ion HI^+, with the $^3\Pi_1$ component and will give rise to its autoionization in the (Π_1) $^2\Pi_{3/2}$ continuum [12]. These types of autoionization concern states having similar potential curves and consequently these interactions appear mainly between states having the same value of v.

2.3. Spin Orbit Autoionization

The interactions so far described involve states of the same spin multiplicity. If, however, the relativistic spin-orbit interaction is introduced, the spin-orbit autoionization can be accounted for. Between Rydberg levels of same value of $\Omega = \Lambda + \Sigma$, a spin-orbit interaction takes place, for example between the $^1\Pi_1$ and $^3\Pi_1$ $(\pi^3\sigma)$ states. Consequently, a state belonging to a Rydberg series, converging to the upper $^2\Pi_{1/2}$ substate of the inverted π^3 $^2\Pi$ ion state, can be autoionized in the continuum of the lower $^2\Pi_{3/2}$ substate [12]. The potential curves corresponding to the two substates can, in a first approximation, be considered as identical. Consequently the vibrational functions are the same for the two spin-orbit components. Thus only states corresponding to the same value of v can interact.

2.4. Vibrational Autoionization

A vibrational autoionization, i.e. a coupling between states corresponding to different values of v, appears as a consequence of the R-dependence of the different types of interactions discussed above. To calculate the vibrational autoionization two different representations of the electronic functions can be used. The diabatic representation used for electronic autoionization in Sect. 2.1 is defined so that the nuclear kinetic energy term is diagonal. The R-dependence of the residual interaction couples on different vibrational levels of two different electronic states giving rise to vibrational diabatic autoionization. Taking the residual interaction as R-independent results in the neglect of a part of the vibrational interaction. This is the model used for CO autoionization discussed in Sect. 4.

In the adiabatic representation the total electrostatic Hamiltonian is diagonalized but we are left with an interaction due to the nuclear kinetic energy operator. This interaction V_{rE} is a vibronic interaction and can be reduced to the following main term:

$$V_{rE} = \langle \chi_v^E(R) | \phi^E(r, R) \frac{d}{dR} \phi^r(r, R) \frac{d}{dR} | \chi_{v'}^r(R) \rangle \qquad (3)$$

We distinguish between pure vibrational autoionization with functions having the same electronic ionic core but different vibrational levels and vibrational adiabatic autoionization when the ionic cores are different. The case of pure vibrational autoionization has been studied in N_2. The $^1\Sigma_u^+$ $p\sigma_u$ Rydberg states converging to the $v+1$ level of the $X^2\Sigma_g^+$ of N_2^+,

are autoionized by the continuum of the v level of the same state [13].

The interaction (3) has been shown [11] to be related to the R-variation of the δ quantum defect, i.e. to the difference between the potential curves of the Rydberg state and of the ion. Equation (3) can be written:

$$V_{rE}=\sqrt{\frac{2\,\mathrm{Ryd}}{n^{*3}}}\left(\frac{\mathrm{d}\delta}{\mathrm{d}R}\right)\langle\chi_v^E(R)\,|R-R_e|\,\chi_{v'}^r(R)\rangle \qquad (4)$$

R_e is the equilibrium internuclear distance, taken the same for the two states.

Other similar vibrational interactions due to the R-dependence of other parts of the Hamiltonian, namely the rotational or the spin orbit parts, can be considered. For the rotational operator, two quantities are dependent on R. The B operator is, in fact, $B(R)=\hbar^2/2\,\mu R^2$, where μ is the reduced mass. A coupling due to centrifugal distortion can appear between the v and $v+1$ states corresponding to the same electronic core. We have in the harmonic approximation:

$$\langle\chi_v^E|\frac{\hbar^2}{2\,\mu R^2}|\chi_{v+1}^r\rangle=2\sqrt{\left(\frac{B_e^3}{\omega_e}\right)}(v+1)^{1/2} \qquad (5)$$

where B_e and ω_e are, respectively, the rotational and harmonic constants of the potential curve. This effect has been implicitly taken into account in H_2 [14]. Another effect is due to the R-variation of the electronic part of either the $L^{\pm}$ or $S^{\pm}$ operator. It is probably rather weak but it is well known in molecular spectroscopy in the case of discrete states. In the present case it would also introduce interactions between different v levels.

The R-variation of the spin-orbit interaction has been taken into account [15] to explain the autoionization of Rydberg states converging to $^2\Pi_{1/2}$ $v=1$ in the continuum of the $^2\Pi_{3/2}$ $v=0$ state of HBr.

3. Theoretical Treatment of the Autoionization

The pioneering works of Berry and Nielsen, in the case of the electronic vibrational autoionization in H_2 [11] and of Duzy and Berry [16], in the case of pure electronic autoionization compared to vibrational autoionization for N_2 [16], have used a golden rule formulation but only obtained the width Γ (Eq. 2) of the autoionized states. There are also results which, starting from close coupling calculations, has introduced the residual electronic interaction as an optical potential and has obtained some results in the case of the autoionization of NO (cf. Collins and Schneider [17]). Other methods have used either the Stieltjes-Tchebycheff method [18] or approaches based on the Kohn variational principle [19] or on the R matrix method type [20–21] and have allowed the calculation of the widths for electrostatic autoionization in the H_2 molecule. Random Phase Approximation with local exchange and electronic correlations has been used in the case of the autoionization of a valence state in C_2H_2 [22]. As yet, no method has used Fano's formulation [7] explicitly for molecules or its extension due to Mies [23]. Many qualitative discussions and interpretations of the experiment have, however, used Fano's formulation. The methods discussed above are devised to calculate ab-initio electronic quantities. They do not treat explicitly the vibrational and rotational part of the interaction except in the case of vibrational autoionizations. A complete procedure must use the total electronic, vibrational and rotational wave functions. Such a procedure is the Multichannel Quantum Defect Theory (MQDT). It goes beyond the analytic formulas such as Eq. (1), which are only valid for two energy states of which one is discrete and the other a continuum. MQDT is able to treat any type of autoionization discussed in Sect. 2. It is based on a number of original concepts which have been reviewed recently [2]. Here we briefly recall the essential ideas. Instead of treating a single Rydberg level, as has been assumed in the above description of autoionization, MQDT uses the original idea of Seaton [24] to treat all discrete members of a Rydberg series and the continuum to which this series converges as a single entity which is called "channel". A channel is defined by the ionic core with its quantum numbers $n^+v^+\Lambda^+$ and the quantum numbers l and λ of the Rydberg or continuum electron. The distinction between bound and continuum states usually introduced in the configuration interaction approach is removed by the extention of the definition of a channel to include the discrete levels. If the energy lies in the discrete region the channel is called a closed channel. Consequently the interactions between individual states are replaced by one interchannel interaction which is defined at any negative or positive electron energy. MQDT defines two regions of space in which the outer electron moves: an internal region which closely surrounds the ionic core and an external or asymptotic region where the ionization (or fragmentation) occurs.

In the internal region, we construct eigenchannel functions which diagonalize the short range Hamiltonian. They form an appropriate representation for the Rydberg levels with low value of n. In this eigenchannel representation, we usually calculate quantum defects and transition moments. The way to per-

form this calculation will be discussed further below. The channels which diagonalize the long range Hamiltonian in the external or asymptotic region are called asymptotic or ionization (or fragmentation) channels. These channels correspond to high n-Rydberg and continuum states since the associated functions extend to large distance. The observables, namely the photoionization cross sections and the photoelectron angular distributions, are written in terms of these channels. This is obvious because the experimental observations take place asymptotically. The link between these two types of functions is obtained by an unitary matrix transformation introduced by Fano [25] and called a frame transformation. This matrix transformation expresses the asymptotic functions in terms of the eigenchannel functions. For example in the case of the spin-orbit autoionization, the $^1\Pi$ and $^3\Pi$ Rydberg states of the neutral molecule expressed by Hund's case (a) functions are finally ionized in the continuum of the $^2\Pi_{1/2}$ and $^2\Pi_{3/2}$ sublevels of the ion expressed by Hund's case (c) functions. Similarly, in the case of the rotational autoionization, the $^1\Sigma^+$ and $^1\Pi$ states of H_2 expressed by Hund's case (b) functions are ionized in the continuum of the $N^+=0$ and $N^+=2$ levels of the H_2^+ ion, described by Hund's case (d) functions. This frame transformation makes it possible to introduce sequentially, and then to treat simultaneously, several types of coupling by taking into account quantum numbers neglected previously: for example, the electronic vibrational autoionization has been treated together with the rotational autoionization in the case of H_2 [26]; also the rotational autoionization has been added to the spin-orbit autoionization in the case of HI [12]. In its standard version MQDT can treat a whole energy region with one energy independent set of electronic quantities (by varying only the photon energy). It allows successive opening of the closed channels since the respective number of closed and open channels is energy dependent.

We have mentioned above what we have to calculate: quantum defects and transition moments. These quantities can be obtained from experiment by a fitting of some accurate spectroscopic data, namely the positions and intensities of the Rydberg states [14]. These fitted electronic quantities are effective quantities which do not correspond to a definite theoretical model. We can also obtain the electronic quantities directly from ab-initio calculations [27] [28], starting from some approximate theoretical model (presently the most common zero order approximation is the single configuration approximation). In fact, the above mentioned procedures are often mixed. The fitting procedure uses at least some information from the calculated potential curves. Ab-initio procedures usually take the ionization potential (which is difficult to calculate accurately) from experiments.

4. Indirect Autoionizations: An Example of Complex and Composite Resonances in the Photoionization Spectrum of CO

In molecules, the supplementary degrees of freedom give rise to numerous possible ionic cores which are often close in energy. To treat the electrostatic interactions due to the continuums associated to all of the vibrational levels of a given electronic state, a sum rule has been used in the preceding works [27] [28]. We have:

$$\Gamma = 2\pi\langle\varphi^r|H|\varphi^E\rangle^2 \Sigma\langle\chi_v^E|\chi_{v'}^r\rangle^2 = 2\pi\langle\varphi^r|H|\varphi^E\rangle^2 \quad (5)$$

and the interaction is consequently reduced to a simple electronic interaction. This is only valid if all vibrational channels are open. In the example given below, only some of the vibrational channels are open and consequently Eq. (5) is not valid. In the 17.0–17.5 eV (730–708 Å) range, the CO photoionization spectrum is perturbed both by the lowest members of the Rydberg series converging to the CO^+ $B^2\Sigma^+$ state (threshold at 19.68 eV) and by the high-n Rydberg states converging to the successive vibrational levels of the $A^2\Pi$ ionic core: the $A^2\Pi$ $v=3$, 4 and 5 thresholds appear respectively at 17.09 eV (725.5 Å), 17.27 eV (717.9 Å) and 17.44 eV (710.9 Å). Three resonant structures are observed experimentally [29] [30]: one at 17.09 eV (725.5 Å), assigned to $(B^2\Sigma^+)\,3'p'\pi\ v=0$ [28] (the first member of the "sharp" series), one at 17.20 eV (721 Å), tentatively assigned by Ogawa and Ogawa [31] to the $n=9$, 10 and 11 Rydberg states associated with the CO^+ $A^2\Pi$ $v=4$ ionic core, and one at 17.30 eV (716.7 Å) which corresponds to the $B^2\Sigma^+$ $3'p'\sigma\ v=0$ and $3'p'\pi\ v=1$ resonances [28].

A theoretical model studying this energy range has to take into account the three ionic states X, A and B and their corresponding vibrational levels. Therefore calculations of the interactions must explicitely account for both electronic and vibrational effects thus giving rise to two types of autoionizations. To study this energy range we have used two models which both neglect pure vibrational autoionization and introduce the vibrational channels with a factorization of the vibrational part. In a preceding work [28] the $v=0$ to 3 and $v=0$ to 1 vibrational levels were introduced for the X and the B states

respectively, but the vibrational levels of the A state were not explicitly taken into account. This approach gave relatively good agreement with the experimental spectrum reproducing the peaks at 17.09 eV (725.5 Å) and 17.30 eV (716.7 Å) which are due to states converging to the $B^2\Sigma^+$ ionic state. However, these calculations were unable to reproduce the observed structure at 17.22 eV (720 Å). The model presented here is an extension of the previous model in that we now include seven vibrational levels for the $A^2\Pi$ ionic core. The Condon factorization of the transition moments and interchannel interactions is, however, still used throughout the calculations.

In these two models, quantum defects, mixing coefficients, transition moments and interactions have been calculated ab-initio except for the second model, where the quantum defects corresponding to the $B^2\Sigma^+$ channels were fitted to the experiment. In MQDT we obtain theoretically a photoionization spectrum calculating the cross section at regularly spaced points in energy. In the second model, due to the very narrow widths associated with high n Rydberg states – the widths within a series decrease as $1/(n-\delta)^3$ where δ is the quantum defect of the series –, we have used a very dense energy grid with a variable step.

In Fig. 1 we display as examples the calculated vibrationally resolved cross sections for the production of CO^+ $X^1\Sigma^+$ $v=0$, 1 and 2. These results have been broadened to a resolution of 0.05 eV to correspond to resolution of the experimental measurements [32]. The main results can be summarized as follows:

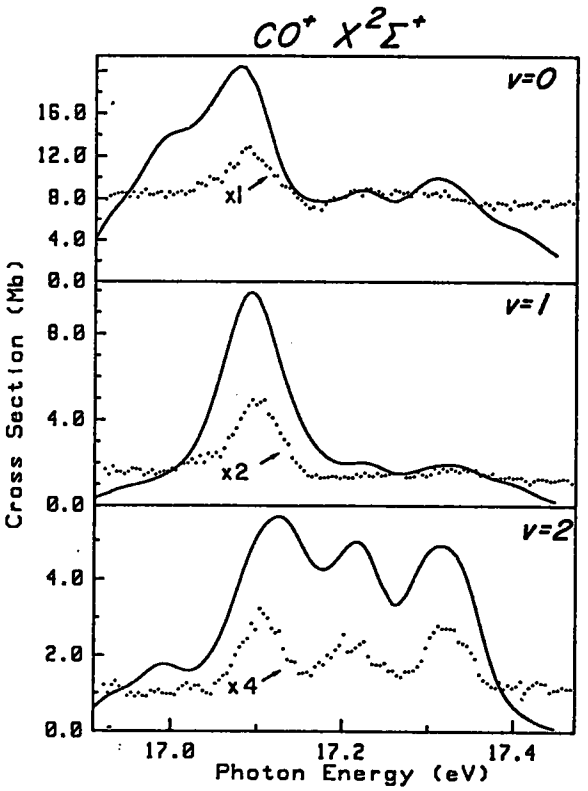

Fig. 1. Vibrationally resolved partial photoionization cross section for production of $v=0$, 1, 2 levels of CO^+ $X^2\Sigma^+$ in the 16.9 to 17.4 eV energy range. Vibrational levels associated with the X, A and B electronic states of the ion have been explicitly taken into account in the calculations. Full lines correspond to theoretical convoluted results. The experimental points are taken from the work of Leyh et al. [32]

(i) The introduction of the vibrational thresholds of the $A^2\Pi$ state results primarily in the emergence of a structure located near 17.22 eV (720 Å). This structure originates in fact from the convolution of a great number of very narrow peaks. The analysis of the spectra reveals that two host series are dominant: $(A^2\Pi \quad v=4)\ n'd'\delta$ and $(A^2\Pi \quad v=4)$ $['(n+1)s+nd']\ \sigma(n>10)$. This partly confirms the assignment of Ogawa and Ogawa [31] but stresses the complexity of molecular photoionization spectra in the vicinity of a vibrational threshold. We shall call this structure a "composite" resonance since it results from the superposition by convolution of a great number of peaks;

(ii) The resonances at 17.09 eV and 17.30 eV are strongly perturbed by the series converging to CO^+ $A^2\Pi$ $v=3$, 4 and 5 and must be considered as "complex resonances" [33] although this fact is not at all straightforward in a low-resolution spectrum. In the complex resonance model [33] the $B^2\Sigma^+ 3'p'\pi$ ($v=0$ and $v=1$) and $3'p'\sigma$ $v=0$ levels appear as broad interlopers in the narrow resonance series converging to the $A^2\Pi$ ionic state. The interaction between these states is such that the interlopers have lost a part of their identity: this means that the assignments given at the beginning of this section are somewhat crude;

(iii) In the vibrationally resolved cross sections of the $X^2\Sigma^+$ state, the intensity ratios between the three resonant structures are in good agreement with experiment for $v=0$ to 2 but not for $v=3$. For $v=3$ level the relative intensity of the intermediate resonance at 17.22 eV (720 Å) is too weak. The theoretical and experimental branching ratios between the $X^2\Sigma^+$ cross sections of different v are also not in good agreement as can be seen in Fig. 1. These discrepancies are perhaps due to the neglect of the pure vibrational autoionization.

5. What Can be Learned from the Comparison between Theory and Experiment

In the case of rovibronic interactions near the first ionization thresholds of H_2 [34], where the electronic quantities have been obtained from either very precise ab-initio calculations or from experimental data, the agreement between theory and experiment is excellent.

The electrostatic and spin-orbit autoionizations so far treated by MQDT rely on ab-initio calculations made in the frozen core static exchange approximation [35]. The agreement obtained has been rather good for the position of the peaks, but the widths and profiles of the peaks occurring in the partial and vibrationally resolved partial cross sections agree only qualitatively with the experiment. There are many reasons for this disagreement. First of all, the model used does not include any correlation (except the autoionizing interaction) for the initial or the final states. This is one reason for which any fitting of the parameters can hide the poorness of the model and the results of such fittings must be used with caution. However, the model provides, in general, a simple interpretation of the experimental data, and detailed understanding of the decay of the Rydberg states in the available channels.

In the case of N_2 [27], CO [28] and HI [12], definite assignments have been given for the autoionizing resonances. For the calculation of the electronic angular distribution, a qualitatively agreement has been obtained for both the electrostatic autoionization of N_2 [27] and the spin-orbit autoionization of HI [36]. However in the case of electrostatic autoionization in CO [28], theory and experiment give inverse structures around 17.09 eV: the experimental maximum of the β curve corresponds to the minimum of the theoretical curve. The reason for this discrepancy is not clear and further calculations and experiments would be very useful.

Other theoretical methods [18–22] have treated electrostatic autoionization (at fixed internuclear distance) introducing supplementary electronic correlations in the initial and final states. However, these results are also only in semi-quantitative agreement with the experiment showing that supplementary work is necessary to obtain a good agreement between theory and experiment.

The number of examples of autoionization features where a comparison between theory and experiment has been made is, unfortunately, very limited. Some new experiments would be useful, for example the determination of the β values in the 700–730 Å wavelength region in the photoionization spectrum of CO [28] or in the 1052–1060 Å wavelength range in the spin orbit autoionization region of HBr [15] for which theoretical predictions already exist. On the other hand new theoretical studies of the autoionized peaks attributed to valence states or of the Auger peaks in inner shell ionization would be very interesting.

The authors thank Dr. A. Giusti-Suzor for useful discussions and to Dr. S.C. Ross for critical reading of the manuscript. B.L. acknowledges NATO (Contract n°96.82), the Belgian Government (Action de Recherche Concertée) and the Fonds de la Recherche Fondamentale Collective (Belgium) for their financial support.

B.L. is indebted to the Fonds National de la Recherche Scientifique (Belgium) for the award of a fellowship.

References

1. a) Dehmer, J.L., Dill, D., Parr, A.C.: In: Photophysics and photochemistry in the vacuum ultra-violet. p. 341 McGlynn, S., et al. (eds.). Dordrecht, Boston, London: D. Reidel Publishing Company 1985;
   b) Dehmer, J.L., Parr, A.C., Southworth, S.H.: In: Handbook on Synchrotron Radiation. Marr, G.V. (ed.), Vol. II. Amsterdam: North Holland 1986
2. Greene, Ch., Jungen, Ch.: Adv. At. Mol. Phys. 21, 51 (1985)
3. Nenner, I., Beswick, J.A.: In: Handbook on synchrotron radiation. Marr, G.V. (ed.), Vol. II. Amsterdam: North Holland 1986
4. Keller, F., Lefebvre-Brion, H.: Z. Phys. D – Atoms, Molecules and Clusters 3 (1986)
5. Southworth, S.H., Parr, A.C., Hardis, J.E., Dehmer, J.L.: Phys. Rev. A 33, 1020 (1986)
6. Holland, D.M.P., Parr, A.C., Ederer, D.L., West, J.B., Dehmer, J.L.: Int. J. Mass Spect. 52, 195 (1983); Hayaishi, T., Iwata, S., Sasanuma, M., Ishiguro, E., Moriaka, Y., Ida, Y., Nakamura, M.: J. Phys. B 15, 79 (1982)
7. Fano, U.: Phys. Rev. 124, 1866 (1961)
8. Bardsley, J.N.: J. Phys. B 1, 349 (1968)
9. Lefebvre-Brion, H., Field, R.W.: Perturbations in the spectra of diatomic molecules. Orlando, Florida: Academic Press 1986
10. Morin, P., Nenner, I., Adam, M.Y., Hubin-Franskin, M.J., Delwiche, J., Lefebvre-Brion, H., Giusti-Suzor, A.: Chem. Phys. Lett. 92, 609 (1982)
11. Herzberg, G., Jungen, Ch.: J. Mol Spectrosc. 41, 425 (1972)
12. Lefebvre-Brion, H., Giusti-Suzor, A., Raseev, G.: J. Chem. Phys. 83, 1557 (1985)
13. Berry, R.S., Nielsen, S.E.: Phys. Rev. A 1, 383, 395 (1970)
14. Jungen, Ch., Atabek, O.: J. Chem. Phys. 66, 5584 (1977)
15. Lefebvre-Brion, H., Dehmer, P.M., Chupka, W.A.: J. Chem. Phys. (to be published) (1986)
16. Duzy, C., Berry, R.S.: J. Chem. Phys. 64, 2431 (1976)
17. Collins, L.A., Schneider, B.I.: Phys. Rev. A 29, 1695 (1984)
18. Hazi, A.U., Derkits, C., Bardsley, J.N.: Phys. Rev. A 27, 1751 (1983)
19. Takagi, H., Nakamura, H.: Phys. Rev. A 27, 691 (1983)
20. Tennyson, J., Noble, C.J.: J. Phys. B 18, 155 (1985)
21. Raseev, G.: J. Phys. B 18, 423 (1985)
22. Levine, Z.H., Soven, P.: Phys. Rev. A 29, 625 (1984)
23. Mies, F.M.: Phys. Rev. 175, 164 (1968)
24. Seaton, M.J.: Proc. Phys. Soc. London 88, 801 (1966)
25. Fano, U.: Phys. Rev. A 2, 353 (1970)

26. Raoult, M., Jungen, Ch.: J. Chem. Phys. 74, 3388 (1981)
27. Raoult, M., Le Rouzo, H., Raseev, G., Lefebvre-Brion, H.: J. Phys. B16, 4601 (1983)
28. Leyh, B., Raseev, G.: Phys. Rev. A (submitted for publication)
29. Huffmann, R.E., Larrabee, J.C., Tanaka, Y.: J. Chem. Phys. 40, 2261 (1964)
30. Berkowitz, J.: In: Photoabsorption, photoionization and photoelectron spectroscopy. p. 228. New York: Academic Press 1979
31. Ogawa, M., Ogawa, S.: J. Mol. Spectrosc. 41, 393 (1972)
32. Leyh, B., Raseev, G., Hubin-Franskin, M.J., Delwiche, J., Lefebvre-Brion, H., Nenner, I., Roy, P., Collin, J.E.: In: Photophysics and photochemistry above 6 eV. p. 33. Amsterdam: Elsevier Science Publishers 1985
33. Giusti-Suzor, A., Lefebvre-Brion, H.: Phys. Rev. A30, 3057 (1984)
34. Jungen, Ch., Dill, D.: J. Chem. Phys. 73, 3338 (1980)
35. Raseev, G.: Comput. Phys. Commun 20, 275 (1980)
36. Carlson, T.A., Gérard, P., Krause, M.O., Vor Wald, G., Taylor, J.W., Grimm, F.A.: J. Chem. Phys. 84, 4755 (1986)

G. Raşeev
H. Lefebvre-Brion
Laboratoire de Photophysique Moléculaire
Bât. 213
Université Paris-Sud
F-91405 Orsay
France

B. Leyh
Département de Chimie Générale
Université de Liège
B-4000 Sart-Tilman par Liège
Belgium